

Scheduling for On-Board Federated Learning with Satellite Clusters

Nasrin Razmi^{*†}, Bho Matthiesen^{*†}, Armin Dekorsy^{*†}, and Petar Popovski^{‡*}

^{*} Dept. of Communications Engineering, University of Bremen, Germany

[†]Gauss-Olbers Space Technology Transfer Center, University of Bremen, Germany

[‡] Dept. of Electronic Systems, Aalborg University, Denmark

Emails: {razmi, matthiesen, dekorsy}@ant.uni-bremen.de, petarp@es.aau.dk

Abstract—Mega-constellations of small satellites have evolved into a source of massive amount of valuable data. To manage this data efficiently, on-board federated learning (FL) enables satellites to train a machine learning (ML) model collaboratively without having to share the raw data. This paper introduces a scheme for scheduling on-board FL for constellations connected with intra-orbit inter-satellite links. The proposed scheme utilizes the predictable visibility pattern between satellites and ground station (GS), both at the individual satellite level and cumulatively within the entire orbit, to mitigate intermittent connectivity and best use of available time. To this end, two distinct schedulers are employed: one for coordinating the FL procedures among orbits, and the other for controlling those within each orbit. These two schedulers cooperatively determine the appropriate time to perform global updates in GS and then allocate suitable duration to satellites within each orbit for local training, proportional to usable time until next global update. This scheme leads to improved test accuracy within a shorter time.

Index Terms—Satellite constellations, low Earth orbit, federated learning, intra-orbit inter-satellite links, scheduling.

I. INTRODUCTION

Mega-constellations of low Earth orbit (LEO) satellites play a crucial role in various applications, ranging from global internet coverage and Earth observation to space exploration [1]–[3]. However, the deluge of data produced by the unprecedented numbers of satellites, e.g., high-resolution hyperspectral images, poses a challenge for transmitting them back to the Earth, particularly considering the limitations on available bandwidth and constraints on delay. Furthermore, specific types of data, e.g., satellite-captured images obscured by clouds, may not be suitable to be sent to the Earth [4].

To tackle these challenges, machine learning (ML) algorithms can be implemented in on-board of satellites to extract valuable insight from the data, leading to reduced needs for communication and improved operational efficiency. A notable example is the Phisat-1, ESA mission [4], which employs a convolutional neural network (CNN) to transmit only non-cloudy images to the Earth, while discarding those with cloud level exceeding a predefined threshold.

This work was funded in part by the German Research Foundation (DFG) under Germany's Excellence Strategy (EXC 2077 at University of Bremen, University Allowance).

978-1-6654-3540-6/22 © 2022 IEEE

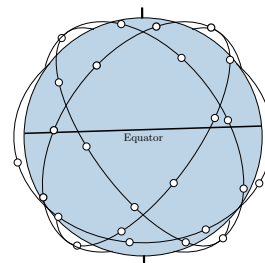


Fig. 1: A satellite constellation with $P = 5$ orbital planes and $K = 40$ satellites. The number of equidistant satellites in all orbits is $K_p = 8$, $\forall p \in \mathcal{P} = \{1, \dots, 5\}$.

To attain an accurate ML model, exploiting data of all satellites is essential. However, constraints such as limited bandwidth impede the sharing of raw data. Here, federated learning (FL) offers a solution by which satellites can collaboratively train an ML model without the need to share the raw data. In canonical FL [5], which is a synchronous scheme, ML model parameters are communicated between the participating clients and parameter server (PS) in several iterations. However, when the clients are satellites, these iterations take longer time due to lack of consistent connection caused by non-visibility periods between the satellites and the PS, located in a ground station (GS), challenging the adoption of FL in satellite constellations [6]. The visibility status of a satellite to a GS forms a pattern called visibility pattern. To deal with the non-visibility periods, an asynchronous FL algorithm is proposed in [7], whose test accuracy is further improved in [8], exploiting the predictability of visibility patterns to schedule the transmissions between satellites and the GS. Subsequently, to make also synchronous FL feasible for satellite constellations, an approach using intra-orbit inter-satellite links (ISLs) is presented in [9] to address the long delay caused by non-visibility periods. This approach requires only one satellite from each orbit to be visible to the GS to access the necessary information from all other satellites in that orbit. Nevertheless, in specific constellations, this approach may not effectively reduce the delay due to the prolonged non-visibility of all satellites in some orbits [10]. Although this particular issue has not been studied in other subsequent works related to satellite FL such as [11]–[14], its

effect can be mitigated by appropriate scheduling, addressed in the current study.

In this paper, as an extension to our previous works [9] and [10], we propose a scheduling scheme that leverages both the predictability of the visibility pattern of each satellite and the cumulative visibility pattern of all satellites within each orbit. The satellites in each orbit are connected together in a ring formation through intra-orbit ISLs. From the GS perspective, the connected satellites are considered as a unified entity, referred to as a cluster. The proposed scheme comprises two schedulers: 1) global update (GU) scheduler and 2) cluster update (CU) scheduler. The GU scheduler, executed at the GS, determines the appropriate time instants for performing global iterations. On the other hand, CU scheduler is responsible to schedule FL procedures within each cluster based on the time instants received from the GU scheduler for global updates, allocating suitable learning duration to satellites within that cluster. The proposed schedulers lead to enhanced accuracy in a shorter duration.

II. SYSTEM MODEL

A. Constellation Configuration

We consider a satellite constellation as Fig. 1 with P orbits and a GS located at a predetermined position on Earth. Each orbit $p \in \mathcal{P} = \{1, \dots, P\}$ is located at an altitude h_p with inclination a_p and contains K_p equidistant satellites denoted by $\mathcal{K}_p = \{k_{p,1}, \dots, k_{p,K_p}\}$. The set of all satellites within the constellation is $\mathcal{K} = \bigcup_{p=1}^P \mathcal{K}_p = \{k_{1,1}, \dots, k_{P,K_P}\}$ with the total number of $K = \sum_{p=1}^P K_p$ satellites.

B. Cumulative Visibility Pattern

At any given time, a satellite in the orbit p may be either visible or non-visible to the GS, depending on their respective locations. The visibility periods are the intervals in which the connection between satellite and the GS is not obstructed by the Earth. In contrast, during non-visibility periods, Earth blocks the line-of-sight (LoS) link between them, resulting in intermittent connectivity. The visibility and non-visibility status of satellite with respect to time is referred to as visibility pattern of that satellite. Here, it is worth mentioning that due to the nature of satellite movements and Earth rotation, the visibility pattern of satellites in any constellation is known in advance.

Satellites in any orbit p as are connected with intra-orbit ISLs form a cluster, denoted by \mathcal{C}_p . Each satellite in \mathcal{C}_p can exchange data, through other connected satellites, with the GS if there is at least one visible satellite to the GS in that cluster. In this regard, we introduce the concept of *cumulative visibility pattern* in which a cluster has a visible status if there is at least one visible satellite to the GS in that cluster.

Fig. 2 shows the cumulative visibility pattern with respect to wall-clock time for a constellation consisting of five orbits $P = 5$, each orbit as a cluster containing eight satellites $K_p = 8$, considering GSs located in two different positions: a) Bremen, Germany, b) São Paulo, Brazil. For the case GS

located in Bremen, we observe that each cluster experiences a visibility period, followed by a prolonged non-visibility period. However, for the other case, with GS in São Paulo, the visibility and non-visibility periods are shorter but occur more frequently. These examples highlight the importance of cumulative visibility patterns in scheduling the procedures of FL for satellite constellations.

C. Communication Model

Each satellite can connect to the GS through ground-satellite link (GSL) and can also communicate with the two nearest neighboring satellites in its orbit via intra-orbit ISLs. To facilitate these connections, each satellite is equipped with three antennas. The GSL antenna is directed toward the Earth's center, while the intra-orbit ISL antennas are positioned on both sides of the satellites, pointing toward the nearest neighboring satellite. Note that we only consider intra-orbit ISLs since inter-orbit ISLs require more complex control [15].

Communication between two satellites k and i is only feasible when there is an unobstructed LoS link between them, meaning that their Euclidean distance, $d_{k,i}$, is less than the maximum slant range $d_{k,i}^S = \sqrt{h_{p(k)}^2 + 2r_E h_{p(k)} + \sqrt{h_{p(i)}^2 + 2r_E h_{p(i)}}$, where $p(k)$ is the orbit index of k -th satellite, and r_E is the Earth radius. Considering GSL, the connectivity between a satellite and the GS is feasible when $\frac{\pi}{2} - \angle(\mathbf{r}_{gs}, \mathbf{r}_k - \mathbf{r}_{gs}) \geq \alpha_e$, where \mathbf{r}_k and \mathbf{r}_{gs} denote the positions of satellite k and the GS respectively, and α_e is the minimum elevation angle [9]. The maximum achievable data rate for ISL transmission between satellites k and i is

$$r_{k,i} = B \log_2 \left(1 + \frac{P_t G_{k,i} G_{i,k} c^2}{16\pi^2 d_{k,i}^2 f_c^2 N_t} \right), \quad (1)$$

where P_t is the transmitted power, $G_{k,i}$ is the antenna gain of satellite k toward satellite i , c is the speed of light and f_c is the carrier frequency. The total noise power is $N_t = k_B B T$ where $k_B = 1.380649 \times 10^{-23}$ J/K is the Boltzmann constant, B and T are the channel bandwidth and the receiver temperature respectively.

The time needed for satellite k to deliver S bits of data to satellite i is obtained by summing up the transmission time and the propagation time as

$$T_{k,i}^C = \frac{S}{r_{k,i}} + \frac{d_{k,i}}{c}. \quad (2)$$

Similar to ISLs, this model can also be applied to the GSLs. For simplicity, we consider the longest distance between each satellite and the GS within visibility period to derive the rate and propagation time.

D. Learning Model

Each satellite k uses its local dataset \mathcal{D}_k to train an ML model, consisting a set of parameters. The overall objective

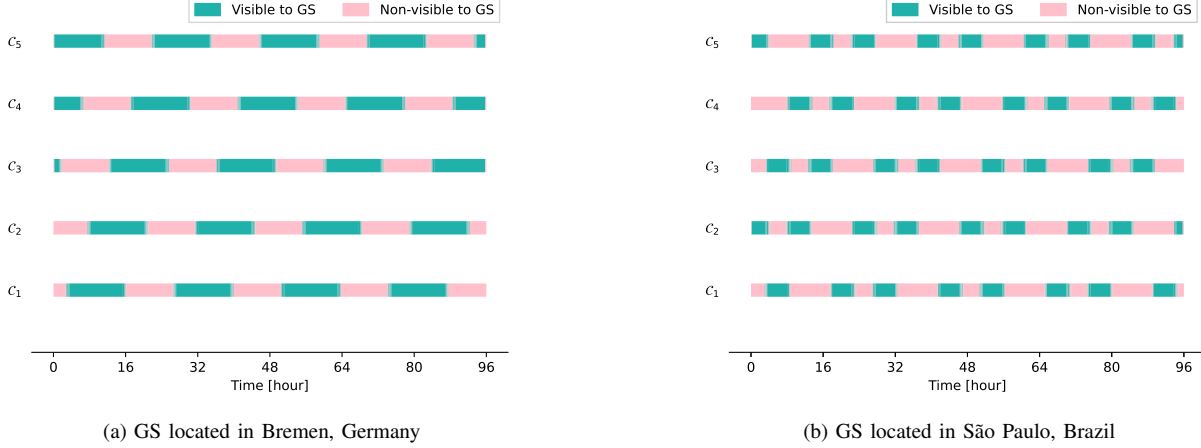


Fig. 2: Cumulative visibility pattern for a Walker Delta constellation with five orbits in an altitude of 2000 km, and inclination 60°, each with eight equidistant satellites considering two GSs: a) located in Bremen, Germany, b) located in São Paulo, Brazil.

Algorithm 1 Satellite Learning Procedure

```

1: procedure SATLEARNPROC( $w^{n-1}$ )
2:   initialize  $w_k^{n-1,0} = w^{n-1}$ ,  $i = 0$ , learning rate  $\eta$ 
3:   for  $I$  epochs do ▷  $I$  epochs of mini-batch SGD
4:      $\mathcal{D}_k \leftarrow$  Randomly shuffle  $\mathcal{D}_k$ 
5:      $\mathcal{B} \leftarrow$  Partition  $\mathcal{D}_k$  into mini-batches of size  $B$ 
6:     for each batch  $\mathcal{B} \in \mathcal{B}$  do
7:        $w_k^{n-1,i} \leftarrow w_k^{n-1,i} - \frac{\eta}{|\mathcal{B}|} \nabla_w (\sum_{x \in \mathcal{B}} f(x, w))$ 
8:     end for
9:      $i \leftarrow i + 1$ 
10:  end for
11:  return  $D_k w_k^{n-1,I}$ 
12: end procedure

```

is to learn the model parameters vector w that minimizes the global loss function $F(w)$ as

$$F(w) = \sum_{k \in \mathcal{K}} \frac{D_k}{D} F_k(w) \quad (3)$$

without sharing the local datasets with the GS or other satellites. The size of dataset \mathcal{D}_k is D_k , and $D = \sum_{k \in \mathcal{K}} D_k$ is the total number of training samples. Moreover, the local loss function of satellite k is

$$F_k(w) = \frac{1}{D_k} \sum_{x \in \mathcal{D}_k} f(x, w), \quad (4)$$

where $f(x, w)$ denotes the loss function for each sample x in the dataset. In overall N global iterations, the GS cooperates with the satellites to minimize (3) [16]. In the n -th iteration, satellite k first receives global model parameters w^{n-1} from the GS. Then, it performs I local epochs of mini-batch stochastic gradient descent (SGD) as Algorithm 1 to minimize (4). It is worth noting that satellites can solve L^2 -regularization loss function $R_k(w, w^{n-1}) = F_k(w) + \frac{\lambda}{2} \|w - w^{n-1}\|_2^2$, where λ is the regularization parameter [16], instead of solving (4). The local model parameters $w_k^{n-1,I}$ are derived and sent back to the GS [7]. Finally, the GS updates the global model

parameters as

$$w^n = \sum_{k=1}^K \frac{D_k}{D} w_k^{n-1,I} \quad (5)$$

and transmits the updated parameters, i.e., w^n , again to the satellites for the next iteration.

III. SCHEDULING SCHEME

As mentioned in the previous sections, intra-orbit ISLs allow satellites to exchange model parameters with the GS through other connected satellites, provided that at least one satellite from their cluster maintains a communication link to the GS. However, this is not always the case as depicted in Fig. 2a. As we can see, the clusters experience long periods of non-visibility, during which no satellite from those clusters are visible to the GS. This becomes problematic, especially when some clusters have completed their training procedures and transmitted their aggregated local model parameters to the GS, while others are non-visible. In such scenarios, the GS has to wait a long period to receive the aggregated local model parameters from all clusters; therefore, performing a global update faces a prolonged delay. To address this issue, one straightforward, but effective, way is to notify the clusters about the timing of the global updates, deduced from the predictability of the cumulative visibility pattern. This will empower the clusters to adjust their allocated time for training appropriately.

To this end, in this section, we introduce a scheduling scheme for satellite FL, comprising two schedulers: 1) a GU scheduler, and 2) a CU scheduler, as depicted in Fig. 3. The GU scheduler, executed at the GS, is responsible to determine the appropriate time instant for each global update in advance, denoted by t_n for the n -th global update. Subsequently, the GS notifies the clusters about this determined instant. Having t_n , the CU scheduler, in each cluster p , derives the feasible duration for local training and accordingly adjusts the appropriate number

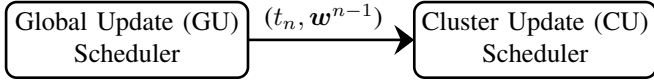


Fig. 3: The time instant for the n -th global iteration, t_n , is calculated by the GU scheduler and along with the global model parameters, \mathbf{w}^{n-1} , are transmitted to the CU schedulers.

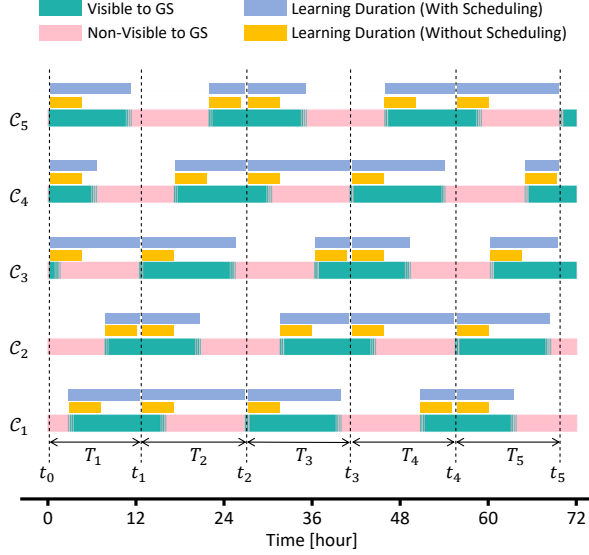


Fig. 4: Comparison of the learning duration between the scheduled and unscheduled schemes in the Walker Delta constellation with five orbits, each containing eight satellites as considered in Fig. 2a.

of local epochs, $I_{n,p}$, that must be performed in the satellites in the n -th iteration. Let define *time slot* as the interval between the instants of two consecutive global updates, denoted by $T_n = t_n - t_{n-1}$ for the n -th global iteration. Consider time slots in the example presented in Fig. 4. The figure shows that when the proposed scheduling scheme is applied, clusters, in each time slot, dynamically adjust their training duration, proportional to their visibility period. However, when this scheduling scheme is not applied, all clusters have to allocate a fixed duration for training in all time slots, leading to extended periods of inactivity in some time slots. In the following, we describe the GU and CU schedulers in detail.

A. Global Update (GU) Scheduler

The role of GU scheduler is to identify the earliest feasible time instant, t_n , at which n -th global update can be executed at the GS. This means all aggregated local model parameters for time slot n , $\mathbf{w}_p^n = \sum_{k=1}^{K_p} \frac{D_k}{D_p} \mathbf{w}_k^{n-1,I}$ where $D_p = \sum_{k=1}^{K_p} D_k$, from any cluster p should be received at the GS by t_n . To this end, the GU scheduler uses the predictability of cumulative visibility pattern on one hand, and the required time to provide the aggregated local model parameters in the clusters on the other hand. The GU scheduler, before the start of the n -th time slot, derives t_n as

$$t_n = \max_p t_{n,p}^F, \quad (6)$$

where $p \in \{1, \dots, P\}$ and $t_{n,p}^F$ is the earliest feasible time instant by which the aggregated local model parameters of cluster p , \mathbf{w}_p^n , can be received at the GS. To formulate $t_{n,p}^F$, at first, the GU scheduler calculates a time instant called *demand time*, $t_{n,p}^D$, for time slot n and cluster p . It is the time instant by which the following procedures within the cluster p are completed: 1) the cluster receives the global model parameters from the GS which demands, as (2), a time interval of $T_{gs,p}^C$, 2) the global model parameters are distributed among satellites in the cluster through intra-orbit ISLs, demanding time interval of T_p^{ISL} , 3) local training is performed in on-board of the satellites which demands a minimum learning duration of T_p^L , 4) the local model parameters are collected and aggregated within the cluster, again through intra-orbit ISLs, demanding time interval of T_p^{ISL} . Hence, the demand time instant, $t_{n,p}^D$, is formulated as

$$t_{n,p}^D = t_{n,p,1}^R + T_{gs,p}^C + T_p^{ISL} + T_p^L + T_p^{ISL}, \quad (7)$$

where $t_{n,p,1}^R$ is the first rise time, in the time slot n , in which the GS sends the global model parameters, i.e. \mathbf{w}^{n-1} , to the cluster p . The m -th rise time in the time slot n , $t_{n,p,m}^R$, is the time instant in which the cluster p for the m -th time becomes visible to the GS. Here, it is worth mentioning that a close observation of the cumulative visibility pattern occasionally shows frequent transitions between visibility and non-visibility states within a short period of time, resulting in having multiple rise and set times within each time slot.

After the above-mentioned procedures, the aggregated local model parameters, \mathbf{w}_p^n , are ready to be transmitted back to the GS if it is feasible, i.e., at least one satellite from the cluster becomes visible to the GS. Therefore, at time instant $t_{n,p}^D$, if the cluster p is in visible state, then it can immediately transmit \mathbf{w}_p^n to the GS, and if it is in non-visible state, then it should wait until the next earliest visibility for transmitting those parameters. Therefore, by considering these two cases, $t_{n,p}^F$ is formulated as

$$t_{n,p}^F = \begin{cases} t_{n,p}^D + T_{p,gs}^C, & \text{if } t_{n,p,m}^R \leq t_{n,p}^D \leq t_{n,p,m}^S \\ t_{n,p,m^*}^R + T_{p,gs}^C, & \text{otherwise} \end{cases} \quad (8)$$

where $t_{n,p,m}^S$ is the m -th set time, the time instant in which the m -th visibility period of the cluster p ends, in the time slot n . In (8), $T_{p,gs}^C$ is the time interval required for transmitting the aggregated parameters from the cluster to the GS. Furthermore, t_{n,p,m^*}^R is the first subsequent rise time after $t_{n,p}^D$, meaning m^* is determined by

$$m^* = \underset{m}{\operatorname{argmin}} t_{n,p,m}^R \quad \text{s.t.} \quad t_{n,p,m}^R \geq t_{n,p}^D. \quad (9)$$

By calculating $t_{n,p}^F$ for all clusters, t_n can be derived using (6), which is transmitted along with the global model parameters, \mathbf{w}^{n-1} , to the clusters by the GS at the beginning of the n -th time slot.

B. Cluster Update (CU) Scheduler

The role of CU scheduler in each cluster is to determine the maximum possible number of local epochs that can be

performed by the satellites of that cluster within each time slot n . To this end, at first rise time in the n -th time slot, i.e. $t_{n,p,1}^R$, the GS transmits \mathbf{w}^{n-1} and next global update time instant, i.e. t_n , to the one visible satellite of the cluster p , referred to as *source*. Then, the source uses t_n and the visibility pattern of satellites in that cluster to calculate the available time, $T_{n,p}^A$, which is the maximum time duration that can be allocated before t_n for local training and communication procedures in the cluster. The time allocated for the communication procedures is for distributing the global model parameters and collecting the updated local model parameters among satellites through intra-orbit ISLs. After performing these procedures, one satellite from the cluster, referred to as *sink*, transmits \mathbf{w}_p^n to the GS when it is in the visible state. Here, two cases are possible: 1) at time t_n , the cluster is visible to the GS, and 2) the cluster is not visible to the GS at that time, t_n . For the first case, the cluster immediately transmits the aggregated model parameters, \mathbf{w}_p^n , to the GS at t_n . However, for the second case, the \mathbf{w}_p^n should be transmitted to the GS at the latest set time before t_n . These two cases are formulated as

$$T_{n,p}^A = \begin{cases} t_n - t_{n,p}^X, & \text{if cluster } p \text{ is visible at } t_n \\ t_{n,p,m^+}^S - t_{n,p}^X, & \text{otherwise} \end{cases} \quad (10)$$

where $t_{n,p}^X = t_{n,p,1}^R + T_{gs,p}^C$, is the time instant in which the source receives the global model parameters from the GS. Moreover, t_{n,p,m^+}^S is the latest subsequent set time before t_n , meaning m^+ is determined by

$$m^+ = \underset{m}{\operatorname{argmax}} t_{n,p,m}^S \quad \text{s.t.} \quad t_{n,p,m}^S \leq t_n. \quad (11)$$

Using the calculated available time, $T_{n,p}^A$, by the source satellite, maximum possible number of local epochs that can be performed by the satellites of the cluster p within time slot n is derived as

$$I_{n,p} = \left\lfloor \frac{T_{n,p}^A - 2T_p^{ISL} - T_{p,gs}^C}{T_p^E} \right\rfloor, \quad (12)$$

where T_p^E is the required time for one local epoch which we, for simplification, assume it identical for all satellites in the cluster p ; however, extending it to the heterogeneous case is straightforward if required. Moreover, $\lfloor \cdot \rfloor$ is the floor function. The upper-bound estimate of $T_p^{ISL} = \left\lceil \frac{K_p}{2} \right\rceil T_{k,j}^C$ is considered, which is the required time duration for distributing the global model parameters among the satellites or, conversely, collecting the local model parameters from them within the cluster, and $\lceil \cdot \rceil$ is the ceiling function. Moreover, $T_{p,gs}^C$ is the time duration required for communicating the aggregated local model parameters from the cluster to the GS. Then, the source determines the sink, a satellite in the cluster which is visible to the GS at time $t_{n,p}^X + T_{n,p}^A$.

After determining $I_{n,p}$ and the sink by CU scheduler, we adopt the same scheme described in [9] for distributing and collecting parameters through intra-orbit ISLs within each cluster. It means the source transmits $I_{n,p}$ and the sink index along with \mathbf{w}^{n-1} to its two nearest neighbor satellites in

both directions in the orbit via intra-orbit ISLs. Then, each receiving satellite forwards these pieces of information to their nearest neighbor satellite in the opposite direction of reception, continuing process until all satellites in the ring cluster have received the information [9]. Each satellite, after forwarding the received global parameters to its neighbor, initiates its learning as Algorithm 1 by setting the number of local epochs to $I_{n,p}$.

Following the algorithm described in [9], the two satellites in the cluster located farthest from the sink, after completing their learning phase, start to transmit the updated local model parameters to their nearest neighboring satellite in direction of the shortest path to the sink. These receiving satellites aggregate the received parameters with their own local updated parameters. Subsequently, they transmit the aggregated model parameters to the next nearest neighboring satellite in the opposite direction of reception. This aggregation and transmission sequence continues until the sink receives the aggregated local parameters from both directions. Finally, the sink aggregates the received parameters with its own parameters, derives \mathbf{w}_p^n and transmits it to the GS. The GS, after receiving the aggregated parameters from all clusters, calculates the global model parameters as $\mathbf{w}^n = \sum_{p=1}^P \frac{D_p}{D} \mathbf{w}_p^n$ and continues with the next iteration.

IV. PERFORMANCE EVALUATION

To evaluate the performance of the proposed scheduling scheme for satellite FL, we perform experiments on a Walker Delta constellation with 40 satellites distributed across five orbits, located at the altitude of 2000 km. The inclination is set to 60° . The GS is situated in Bremen, Germany, with a minimum elevation angle of 10° . For the communication links, we set $f_c = 20$ GHz, $B = 500$ MHz, $P_t = 40$ dBm, $T = 354$ K, and the antenna gains are set to 32.13 dBi [17].

A deep CNN with 122 570 parameters [18] is trained on the CIFAR-10 dataset, which contains 60 000 color images with the size of 32×32 , categorized in ten classes. The dataset distributed among satellites in a non-independent and identically distributed (non-i.i.d) manner using the Dirichlet distribution with a concentration parameter of 0.5 [19], [20]. The batch size is 10, and the learning rate η and regularization parameter λ are set to 0.1 and 0 respectively. The time to complete a local epoch is set to 1 hour. Moreover, the minimum demanded learning duration is set as the time needed to complete one local epoch by the satellites, i.e. $T_p^L = T_p^E$. The simulation is conducted using the FedML library [21].

In Fig. 5, we compare the test accuracy between our proposed scheduling scheme and the scheme without scheduling in terms of wall-clock time. Unlike the proposed scheme which dynamically adjusts the number of local epochs, $I_{n,p}$, for each cluster p and time slot n , the scheme without scheduling assigns a fixed number of local epochs, I , to satellites in all time slots. We evaluate three different cases for the scheme without scheduling: 1) two local epochs, i.e., $I = 2$, 2) eight local epochs, i.e., $I = 8$ and 3) ten local epochs, i.e., $I = 10$.

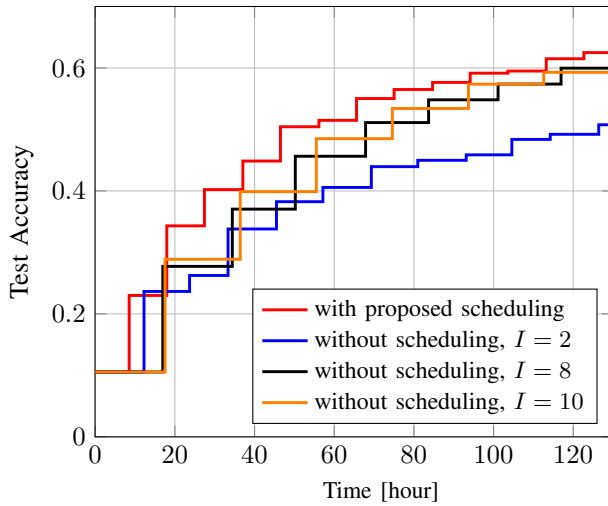


Fig. 5: Test Accuracy of the proposed scheme with scheduling, with respect to wall-clock time, is compared with the scheme without scheduling for a Walker Delta constellation, comprising five orbits, each with eight satellites. In the scheme without scheduling, I is the number of local epochs in each iteration and is fixed, while the scheme with scheduling dynamically adjusts this value based on the available time for each orbit in each time slot.

The proposed scheme achieves higher accuracy compared to the scheme without scheduling for all the cases. Considering the case without scheduling with a lower I , e.g. $I = 2$, the improvement achieved by the proposed scheme is attributed to the increased number of local epochs, $I_{n,p}$, in some clusters and time slots. The proposed scheme assigns $\{I_{1,1} = 5, I_{1,2} = 1, I_{1,3} = 1, I_{1,4} = 6, I_{1,5} = 8\}$ to the clusters in the first time slot, and for the second time slot, it sets $\{I_{2,1} = 7, I_{2,2} = 9, I_{2,3} = 5, I_{2,4} = 1, I_{2,5} = 2\}$. This indicates the dynamic adjustment of $I_{n,p}$ for different p and n results in having higher number of local epochs than the fixed $I = 2$ on average.

On the other hand, when considering the case without scheduling with a higher I , e.g. $I = 10$, the improvement achieved by the proposed scheme is attributed to the increased number of global updates within given period of time. The proposed scheme adjusts $I_{n,p}$ to lower values for those clusters that become visible to the GS at a later time in each iteration. This prevents global updates from being delayed due to lack of local model parameters of those clusters, thus allowing for more frequent global updates. For example, in the second time slot, as we mentioned above, $I_{2,4} = 1$, allowing the fourth cluster to transmit its local model parameters to the GS without long delay, despite becoming visible to the GS at a later time. However, in the scheme without scheduling, the absence of the dynamic adjustment results in the prolonged delays, as all clusters, even those experiencing delay, undergo the same high number of local epochs in all iterations.

V. CONCLUSION

We have presented a scheduling scheme to enable efficient federated learning in satellite constellations connected with intra-orbit inter-satellite links. Our approach leverages the predictability of visibility of each satellite as well as the

cumulative visibility of all satellites in each orbit to effectively address intermittent connectivity challenges. The proposed scheme incorporates two main schedulers: one for controlling the global update times and the other for managing learning procedures within each orbit. The scheduling scheme has enhanced the test accuracy by determining the appropriate time instants for global updates and dynamically adjusting the number of local epochs for each orbit and iteration, as confirmed by simulation results.

REFERENCES

- [1] I. Leyva-Mayorga *et al.*, "LEO small-satellite constellations for 5G and beyond-5G communications," *IEEE Access*, vol. 8, 2020.
- [2] S. Liu *et al.*, "LEO satellite constellations for 5G and beyond: How will they reshape vertical domains?" *IEEE Commun. Mag.*, vol. 59, no. 7, pp. 30–36, 2021.
- [3] H. Luo *et al.*, "Very-low-earth-orbit satellite networks for 6G," *Commun. Huawei Res.*, pp. 40–53, 2022.
- [4] G. Giuffrida *et al.*, "Cloudscout: a deep neural network for on-board cloud detection on hyperspectral images," *Remote Sensing*, vol. 12, no. 14, p. 2205, 2020.
- [5] B. McMahan, E. Moore, D. Ramage, S. Hampson, and B. Agüera y Arcas, "Communication-efficient learning of deep networks from decentralized data," in *Artif. Intell. Statist. (AISTATS)*, FL, USA, Apr. 2017.
- [6] B. Matthiesen, N. Razmi, I. Leyva-Mayorga, A. Dekorsy, and P. Popovski, "Federated learning in satellite constellations," *IEEE Netw.*, 2023, early access.
- [7] N. Razmi, B. Matthiesen, A. Dekorsy, and P. Popovski, "Ground-assisted federated learning in LEO satellite constellations," *IEEE Wireless Commun. Lett.*, vol. 11, no. 4, pp. 717–721, 2022.
- [8] —, "Scheduling for ground-assisted federated learning in LEO satellite constellations," in *Eur. Signal Process. Conf. (EUSIPCO)*, Belgrade, Serbia, Aug. 2022.
- [9] —, "On-board federated learning for dense LEO constellations," in *IEEE Int. Conf. Commun. (ICC)*, Seoul, Korea, May 2022.
- [10] —, "On-board federated learning for satellite clusters with inter-satellite links," <https://arxiv.org/abs/2307.08346>, 2023.
- [11] M. Elmahallawy and T. Luo, "FedHAP: Fast federated learning for LEO constellations using collaborative HAPs," in *2022 14th International Conference on Wireless Communications and Signal Processing (WCSP)*, 2022, pp. 888–893.
- [12] J. Östman, P. Gomez, V. M. Shreenath, and G. Meoni, "Decentralised semi-supervised onboard learning for scene classification in low-earth orbit," *arXiv preprint arXiv:2305.04059*, 2023.
- [13] C.-Y. Chen, L.-H. Shen, K.-T. Feng, L.-L. Yang, and J.-M. Wu, "Edge selection and clustering for federated learning in optical inter-LEO satellite constellation," <https://arxiv.org/abs/2303.16071>, 2023.
- [14] J. So *et al.*, "FedSpace: An efficient federated learning framework at satellites and ground stations," *arXiv preprint arXiv:2202.01267*, 2022.
- [15] B. Soret, I. Leyva-Mayorga, and P. Popovski, "Inter-plane satellite matching in dense LEO constellations," in *2019 IEEE Global Commun. Conf. (GLOBECOM)*, 2019, pp. 1–6.
- [16] T. Li *et al.*, "Federated optimization in heterogeneous networks," *arXiv preprint arXiv:1812.06127*, 2018.
- [17] I. Leyva-Mayorga *et al.*, "NGSO constellation design for global connectivity," in *Non-Geostationary Satellite Communications Systems*, E. Lagunas, S. Chatzinotas, K. An, and B. F. Beidas, Eds. Hertfordshire, UK: IET, Dec. 2022, ch. 9, pp. 189–236.
- [18] Y. Fraboni, R. Vidal, L. Kameni, and M. Lorenzi, "A general theory for federated optimization with asynchronous and heterogeneous clients updates," *J. of Mach. Learn. Res.*, vol. 24, no. 110, pp. 1–43, 2023.
- [19] M. Yurochkin *et al.*, "Bayesian nonparametric federated learning of neural networks," in *ICML*, California, USA, Jun. 2019.
- [20] H. Wang, M. Yurochkin, Y. Sun, D. Papailiopoulos, and Y. Khazaeni, "Federated learning with matched averaging," in *Int. Conf. Learn. Repr. (ICLR)*, Apr. 2020.
- [21] C. He *et al.*, "Fedml: A research library and benchmark for federated machine learning," *arXiv preprint arXiv:2007.13518*, 2020.